

Energy & mass-charge distribution peculiarities of ion emitted from penning source

N V Mamedov¹, D V Kolodko², I A Sorokin², I A Kanshin¹ and D N Sinelnikov²

¹Federal State Unitary Enterprise “All-Russian Research Institute of Automatics n.a. N.L. Dukhov”, Sushchevskaya st. 22, Moscow, Russia, 127055,

²National Research Nuclear University MEPhI (Moscow Engineering Physics Institute), 31 Kashirskoe sh., 115409 Moscow, Russia

E-mail: m_nikitos@mail.ru

Abstract. The optimization of hydrogen Penning sources used, in particular, in plasma chemical processing of materials and DLC deposition, is still very important. Investigations of mass-charge composition of these ion source emitted beams are particular relevant for miniature linear accelerators (neutron flux generators) nowadays. The Penning ion source energy and mass-charge ion distributions are presented. The relation between the discharge current abrupt jumps with increasing plasma density in the discharge center and increasing potential whipping (up to 50% of the anode voltage) is shown. Also the energy spectra in the discharge different modes as the pressure and anode potential functions are presented. It has been revealed that the atomic hydrogen ion concentration is about 5-10%, and it weakly depends on the pressure and the discharge current (in the investigated range from 1 to 10 mTorr and from 50 to 1000 μ A) and increases with the anode voltage (up to 3,5 kV).

1. Introduction

As is known, the penning hydrogen ion sources are widely used in plasma chemical processing of materials and deposition of diamond-like thin films, that is why the optimization of operation modes of this kind of sources is still extremely important. The studies of the component composition of the beam extracted from a miniature linear accelerator used to generate neutron fluxes (using D-D or D-T reactions) are also relevant.

Over the last decades, compact neutron generators (NG) are more and more used in various fields of science and technics due to their reliability, radiation safety and easy operation [1]. One of the main elements of NG is the neutron tube (NT) – vacuum neutron tube (VNT) and gas-filled neutron tube (GNT). Despite the obvious advantages of GNT (wide frequency range of neutron pulses generation, the stable neutron flux throughout the lifetime) the increase in the neutron yield and the lifetime are still extremely relevant. As is known, the neutron yield is affected by two main factors – the characteristics of the ion source (IS) (usually used penning type) and properties of target materials. The various options for optimizing the geometric parameters of the bit cell source to increase the discharge current and, as a consequence, to increase the drawn ion current are shown in [2-5]. High neutron output is limited also by the low atomic ions concentration of deuterium (or tritium) when using penning ion source as compared with the molecular one. In [5, 6] the effect of electrode materials on the discharge characteristics and the mass-charge composition has been studied. For example, it is shown that the use of an aluminium with a boron nitride layer as an electrode material



increases the proton component ratio up to 16%, but also leads to discharge instabilities such as film sputtering.

As one knows, a low number of atomic ions for the hydrogen discharges is a consequence of the low electron density and short life time of molecular ions H_2^+ [5,7]. The lifetime of ions is directly related to the recombination coefficient, i.e. the materials of the electrode surface [5]. Thus, the increased electron density at least in a local region of the discharge (for example, by changing the discharge combustion mode) can significantly change the mass-charge ratio of the extracted ion beam.

2. Experimental setup description

The high vacuum setup designed in the NRNU MEPhI for the penning ion source main parameters measurements is shown in figure 1. The source (1), fixed by Teflon rings (2), is isolated from the ground potential of the setup. Thus, in addition to the anode potential ($U_d < 4\text{ kV}$) the bias potential relative to ground ($U_{ex} < 15\text{ kV}$) can be set to the source casing.

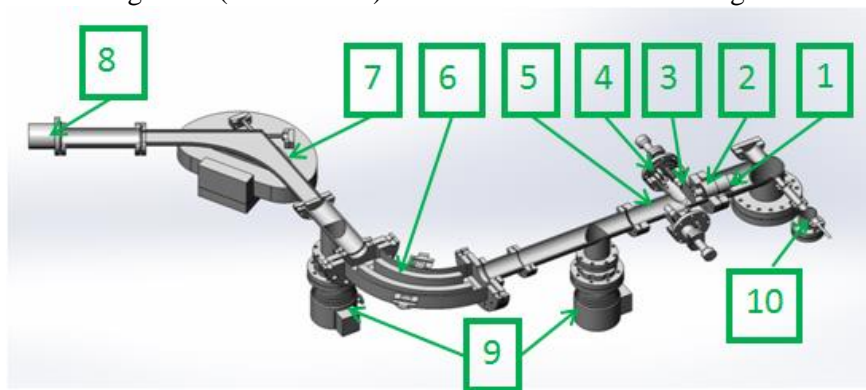


Figure 1 Schematic of the experimental setup (description in the text).

Plate (3) with a circular aperture 1,6 mm diameter is located on the precious linear motion feedthrough (4) in front of the ion source exit orifice at a 5 mm distance. Plate is grounded through an ammeter, which measures the total current of the extracted beam. It is the accelerating electrode at the same time. Measuring probe $2.5 \times 3 \text{ mm}^2$ (5) is mounted at a 50 mm distance from the plate on the same feedthrough. Changing the position of the diaphragm (3) and the probe (5) and measuring the current by ammeter, the spatial distribution of the ion beam and emittance are determined.

Henceforth the extracted ion beam enters the quarter-spherical electrostatic deflector (6) with the energy resolution from 0.8% to 1.5% [8]. The ions passing energy analyzer are registered by the Faraday Cup, (installed on a movable input) or fly into a magnetic mass-monochromator (7). This device permits one to separate the ions with mass to charge ratios of up to $M/Z = 40$; maximum beam energy of up to 10 keV and mass resolution $M/\Delta M \leq 30$ (for 5keV ion beam) [9]. After that the ion beam current is measured by secondary electronic multiplier VEU-1A (8). The recovery of the energy spectra (and similarly mass spectra) takes place automatically in the control program according to the method described in [10].

The vacuum system consists of two turbomolecular pumps Pfeiffer HiPace 80 (9). Working gas is introduced directly into the source volume through a Teflon tube with the precious leak (10). The working pressure in the interaction chamber, (as measured by the pressure sensor Pfeiffer PKR 251,) was of an order of $10^{-3} - 10^{-4}$ Torr, the maximum residual vacuum of the order of $\sim 10^{-6}$ Torr. The gas pressure in the source is calculated according to the Pfeiffer gauge PKR 251 data taking into account the conductivity of the source output aperture and the pumping speed.

The size of the investigated ion source is about $20 \times \varnothing 15 \text{ mm}$. Magnetic field is uniform in the center of the cell and has a value of 100 mT. Comsol Simulation of potential distribution on its axis depending on the anode voltage U_d was done.

3. Experimental results and discussion

Before the beginning of the experiments the setup has been evacuated during 3 hours to the ultimate vacuum. Then during 10 to 30 minutes the source has been heated and degassed on exposure to its

own discharge (the anode voltage $U_d = 2$ kV, the pressure $P = 5$ mTorr and the discharge current of the order of $I_d = 600$ μ A).

Current-voltage characteristics of the discharge at different pressures inside the source are shown in figure 2. As can be seen from the plot data the discharge characteristic shows sharp jumps at pressures above 5 mTorr and then the discharge current increases slowly and smoothly provided the anode voltage increases. To explain this feature one can use the results of the [11]. Because the ion density is proportional to the gas density, there exists the critical pressure at which the ion density on the inner boundary of the plasma sheath becomes comparable with the electron density. Under the assumption of the electron density finiteness the pressure increase above this level leads to the disappearance of the anodic sheath.

It has been shown [11] that the dependence of the critical pressure on the anode voltage is expressed by a power function with an index between -0.5 and -1. Thus, for certain combinations of magnetic field, pressure and anode voltage at the moment of the transition to another mode of the discharge the potential in the cathode region decreases. In the central region of the anode a dense plasma forms. This explanation qualitatively agrees with experiments [12] that have photos of the discharge at various anode voltages during the current-voltage characteristics measurements. Those photos show that the current jumps correlate well with the change in the shape and area of the discharge.

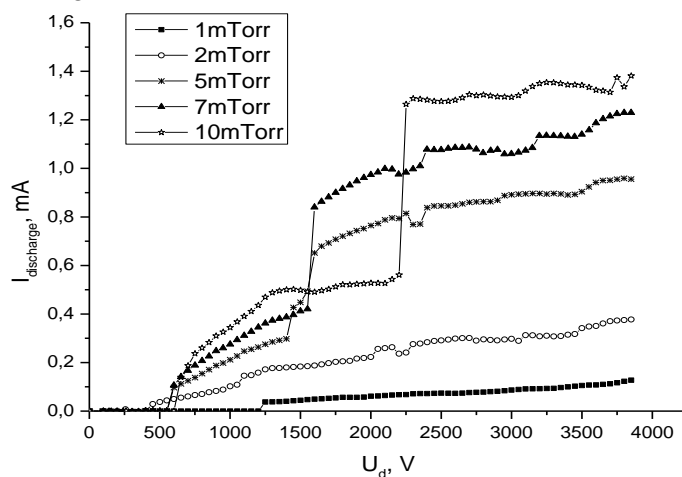


Figure 2. Current-voltage characteristics of the discharge at different pressures inside the source.

A set of extracted ions energy spectra at different voltage on the anode (in this case the source case has been grounded) and at different pressures is presented in Fig. 3-5. Values at the maximum energy of the spectrum are indicated on top of the energy spectra. As can be seen on the "low pressure" graphs (figure 3) the spectra have an asymmetric shape. The sharp growth is observed at the left of the maximum, whereas at the right – the exponential decline (high energy tail). These data are qualitatively similar to Ar energy spectra [13, 14]. Thus, the general form of the spectra (figure 3) can be interpreted as follows. Along the source axis in the discharge region there is no apparent potential difference. All ions generated in this area gain about the same energy reaching the output aperture of the ion source. Thus, due to the anode potential whipping on the axis of the source the energy spectrum of emitted ions shifts to low energy region. "Exponential fall tail" can be explained by the fact that the ion extraction area is not a point and has a finite radial dimension. Therefore, part of ions produced at different equipotential within the boundary layer of the plasma, acquire an energy different from the plasma volume ion one.

As can be seen in figures 4-5 in the transition region at pressures $P \geq 5$ mtorr the energy spectra are shifted to the far low-energy region. There is a noticeable broadening of the spectra, the peak intensity maximum of the spectrum decreases. There are additional low-energy peaks with intensity by order of magnitude smaller than the main peak (see figure 4). The obtained results are similar to the data from [15]. An additional experiment has been carried on to prove that the additional peaks are associated

with the ions also emitted from the ion source. The source body has been biased relative to the earth (up to 1kV). As a result, the whole energy spectrum as a whole shifts to the right by the applied accelerating voltage magnitude.

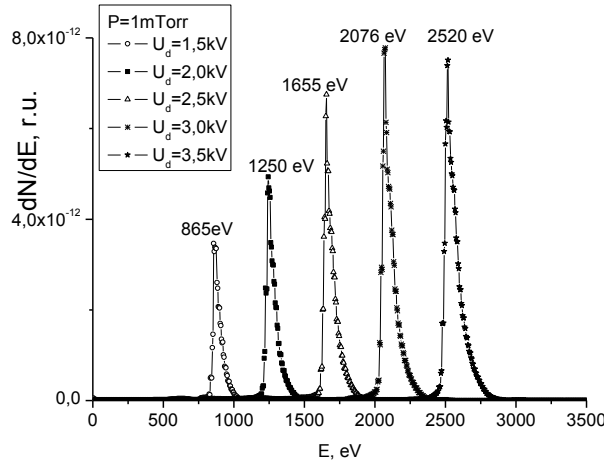


Figure 3. Energy spectra of extracted ions at different anode voltage at pressure $P = 1$ mTorr.

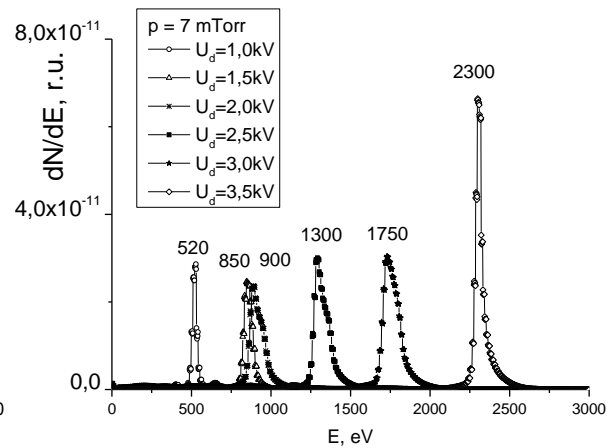


Figure 4. Energy spectra of extracted ions at different anode voltage at pressure $P = 7$ mTorr.

In the transition region (at pressure $P = 7$ mTorr and the anode voltage 1.5-2.0 kV) the discharge can "jump" from one combustion mode to another and back again that is demonstrated by change in the shape and position of the energy spectrum. It should be noted that "two hump" shape of energy spectra appearances at the discharge voltage of 1.5-2.0 kV (see figure 4, 5). With further increase in voltage discharge spectra become more monoenergetic once again (see figure 5), with the only difference from the spectra of figure 3 that in figure 5 spectra there are low-energy peaks.

The potential whipping dependence (the difference between the applied voltage to the anode and the maximum in the resulting energy spectrum $\Delta U = U_d - E_{\max}/e$) on the anode voltage at different pressures is shown in figure 6. It is seen that at low pressures ($P < 5$ mTorr) the potential whipping grows linearly with increasing applied voltage, whereas at higher pressures a sharp increase in the magnitude occurs and then this value reaches the plateau.

Based on [11], photos [12] and the measured energy spectra, one can conclude that after the ignition discharge continuously goes out from T mode (Townsend region) to LMF mode (low magnetic field), i.e. at small B and increasing gas density (pressure). The potential distribution is distorted by a cloud of negative charge existing throughout all volume of the discharge cell. There is a transition mode (TM) at high pressures ($P \geq 5$ mtorr), but the transition to the high pressure mode (HP) is not observed. Cathode layer forms; central plasma is still present; the potential whipping increases.

An overview of the extracted ion mass spectrum at a pressure of 7 mtorr and the discharge voltage 3.5 kV without additional accelerating voltage is presented in figure 7. Each peak is signed with corresponding weight. As can be seen, typical component composition ions emitted from penning source are $H^+ \sim 6\%$, $H_2^+ \sim 90, 5\%$, $H_{2-1}^+ \sim 1,4\%$, $H_2^+(\text{energy}) \sim 0,2\%$, $H_3^+ \sim 0,3\%$, $OH^+ \sim 0,2\%$, $H_2O^+ \sim 0,8\%$, $N^+ \sim 0,08\%$, $O^+ \sim 0,09\%$. H_{2-1}^+ - molecular ions, collapsed during beam transport before entering the magnetic mass separator. H_2^+ (energy) peak of the molecular ions, whose energy spectrum is shifted to the left of the main peak and has an order of magnitude lower intensity (as, for example, in figure 8). The amount of impurity ions (water, oxygen, and nitrogen) is less than 1.5% in all experimental data.

The dependences of the atomic/molecular ions extracted from the ion sources ratio ($\delta = \frac{H^+}{H^+ + H_2^+}$) on the anode voltage at different working gas pressure based on the obtained data are made. As can be

seen from figure 8, the atomic ions fraction is in the range of 5-10%. As a whole there are no fundamental differences of the atomic/molecular ratio on the pressure and discharge current in the specified range. The atomic/molecular ratio increases with increasing anode voltage.

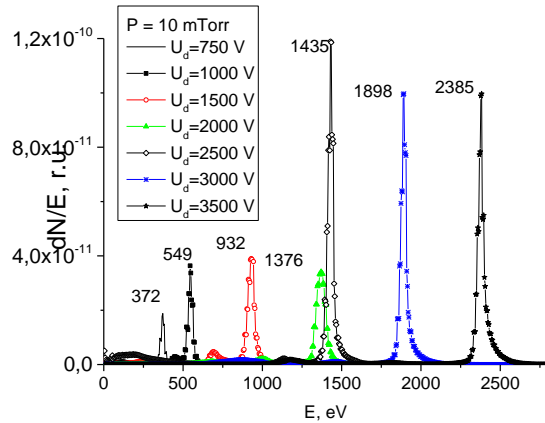


Figure 5. Energy spectra of extracted ions at different anode voltage at pressure $P = 10$ mTorr.

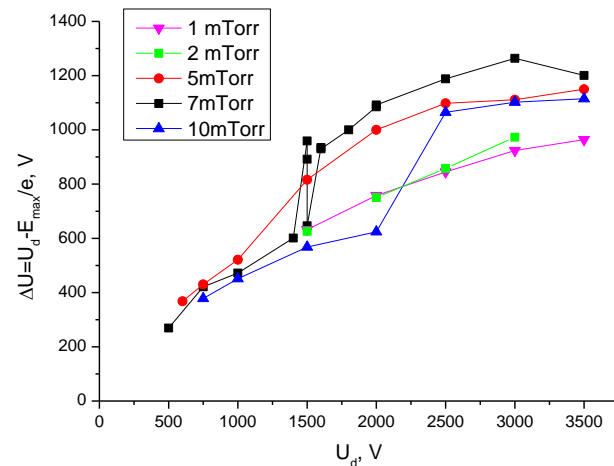


Figure 6. The potential whipping dependence on the anode voltage at different pressures.

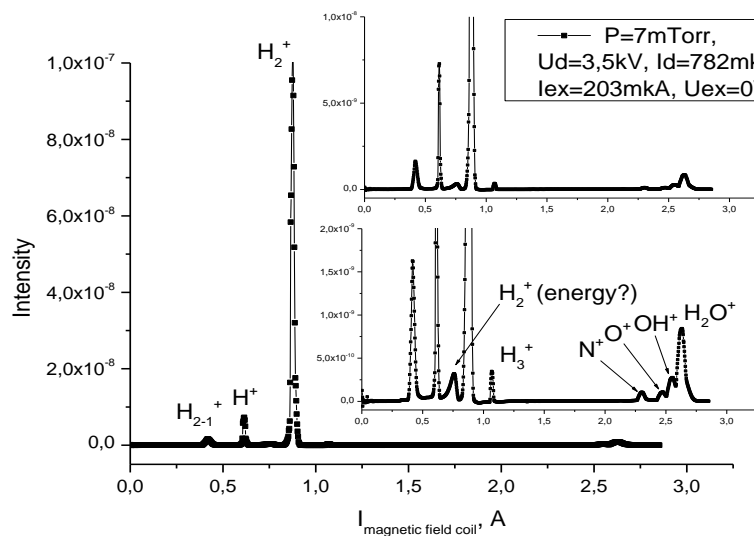


Figure 7. Review of the mass spectrum at a pressure of 7 mtorr and the discharge voltage 3.5 kV.

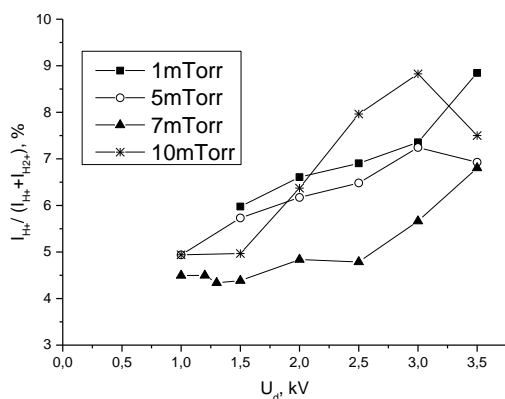


Figure 8. The dependences of atomic/molecular ratios of ions extracted from the penning sources on the anode voltage at different working gas pressure.

4. Conclusion

Investigations of energy distributions and molecular composition of the ions emitted from a penning source are carried out. Current-voltage characteristics for different working gas pressure are measured. It is shown that at pressures above 5 mTorr there are abrupt fluctuations of the discharge current, and then the smooth slow growth with the anode voltage increase. Current ‘jumps’ are explained by the plasma density and potential whipping increase in the center of the discharge. Shapes of the energy spectra depending on the mode of discharge are investigated. The values of the potential inside the source at different pressures and anode voltages are defined. Component composition of the extracted ion beam is measured. The atomic ions fraction is in the range of 5-10%, depends weakly on pressure and discharge current (in the investigated range from 1 to 10 mTorr and from 50 to 1000 μ a) and increases with increasing anode voltage (from 1 to 3.5 kV).

References

- [1] Valkovic V 2016 *14 MeV Neutrons. Physics and Applications* (CRC Press Taylor&Francis Group, Boca Raton, London, New York), 500 p
- [2] Das B K, et al. 2012 *Nuclear Instruments and Methods in Physics Research A* **669** 19
- [3] Liu W, et al. 2014 *Nuclear Instruments and methods in Physics Research A*, **768** 120
- [4] Rovey J L, Ruzic B P, Houlahan T J 2007 *Rev. of Sci. Instrum.* **78** 1
- [5] Sy A, Ji Q, Persaud A, Waldmann O, Schenkel T 2012 *Rev. of Sci. Instrum.* **83** 1
- [6] Ludewight B, et al. 2011 *Neutron Source R&D – from Compact Generators to Neutron Beams* (Proceedings of FNDA)
- [7] Chen F K 1984 *J. Appl. Phys.* **56** 3191
- [8] Mamedov N V, Kurnaev V A, Sinelnikov D N, Kolodko D V 2015 *Instruments and Experimental Techniques* **58(1)** 43
- [9] Kolodko D V, et al. 2014 *Proceedings of 20th International Workshop on Beam Dynamics and Optimization* (Saint Petersburg), p. 87
- [10] Kurnaev V A., Urusov V A 2010 *Technical Physics Letters* **36(5)** 454
- [11] Schuurman W 1967 *Physica* **36** 136
- [12] Mamedov N V, Schitov N N, Kanshin I A 2015 *Physical-Chemical Kinetics in Gas Dynamics* **16(4)** 590
- [13] Rohwer P, et al. 1982 *Nuclear Instruments and methods* **204** 245
- [14] Rohwer P, et al. 1983 *Nuclear Instruments and methods* **211** 543
- [15] Nagy J L 1965 *Nuclear Instruments and methods* **32** 229

Acknowledgments

These studies have been supported by RFBR grant №12-02-13510-OFI_M_RA and have been done in NRNU MEPhI in collaboration with VNIIA. The authors would like to thank Dr. N.N. Schitov from Dukhov All-Russia Research Institute of Automatics for the help and useful discussions.